

## Dielectric and Electric Modulus Study of $Y_{0.85}Gd_{0.15}CrO_3$ Nanoparticles

Ranjita Sinha<sup>1\*</sup>, Sandip Haldar<sup>1</sup>, Soujanya Sengupta<sup>2</sup>, Monalisa Halder<sup>3</sup>, Piyali Saren<sup>4</sup>, Chandan Kumar Raul<sup>5</sup>, Soumen Basu<sup>5</sup>, Ajit Kumar Meikap<sup>5</sup>

<sup>1</sup>Department of BS&HU(Physics), Asansol Engineering College, Asansol-713305, India

<sup>2</sup>4<sup>th</sup> year B.Tech Student, Department of Electronics and Communication Engineering, Asansol Engineering College, Asansol-713305, India.

<sup>3</sup>Department of Basic Science and Humanities, Abacus Institute of Engineering and Management, Mogra-712148, India

<sup>4</sup>1<sup>st</sup> year Diploma Student, Department of Computer Science and Technology, Abacus Institute of Engineering and Management, Mogra-712148, India

<sup>5</sup>Department of Physics, National Institute of Technology, Durgapur-713209, India

Email: [sinha.ranjita15@gmail.com](mailto:sinha.ranjita15@gmail.com)

### Abstract

In this research work  $Y_{0.85}Gd_{0.15}CrO_3$  nanoparticles are synthesized following sol-gel method. Characterization is done by XRD, TEM measurements. XRD pattern proves the well crystalline characteristics and TEM image gives the nanocrystalline nature. Frequency dependence of the dielectric permittivity is estimated for different temperatures in the span of 20 Hz to 2 MHz. The dielectric relaxation spectra using electric modulus formalism is analysed for the sample. Following the electric modulus formalism relaxation time is calculated. Ac activation is also calculated by applying Arrhenius law. The  $M''/M''_{max}$  vs frequency graph for different temperatures shows that all dynamical process taking place for individual temperatures have same activation energy.

**Keywords:** Sol-gel method, Dielectric permittivity, Nanoparticles.

### 1. Introduction

If the association of any two or more ferroic orderings namely ferroelectric, ferromagnetic and ferroelastic are noticed at the same phase inside a material then it is termed as multiferroic material [1-3]. The ferroelectric property in the material can be modified using its conjugate field. For multiferroic material electric polarization may be tuned by magnetic field and also magnetization can be controlled by the application of the electric field. In the 19<sup>th</sup> century the journey of multiferroic material started by Pierre Curie [4]. In the recent time Yttrium Chromite has been reported as a biferroic material inholding weak

ferromagnetism below 140 K ( $T_N$ ) and ferroelectric transition temperature  $T_c$  of 473K having the hysteresis loop [5]. Yttrium Chromite possesses high thermal, chemical and structural stability and also very high melting temperature ( $\sim 2290^\circ\text{C}$ ) [6-8]. Its electrical conductivity is also very high [9]. Due to all these properties  $\text{YCrO}_3$  is very useful candidate for technological demanding different applications namely interconnect material in SOFC, oxidation catalysis, humidity sensor, thermistors and different magnetoelectric field [10-14]. Considering the importance of the material we have doped Gadolinium in Yttrium Chromite to enhance its electrical properties. Here we have discussed the formation, characterization of Gd doped yttrium Chromite. The dielectric and electric modulus formalisms are discussed in detail which is very much important for its technological applications.

## 2. Synthesis Procedure

For the synthesis of Gadolinium doped Yttrium Chromite  $\text{Y}_{0.85}\text{Gd}_{0.15}\text{CrO}_3$  we have taken starting material as (i) Yttrium nitrate hexahydrate (ii) Chromium nitrate nonahydrate and (iii) Gadolinium nitrate hexahydrate. Precursor solution is produced by mixing these weighted materials in distilled water. The PVA solution is poured to the previous mixture with stirring without break. Next the whole solution is kept for evaporation and then dried at  $80^\circ\text{C}$ . The dried powder is calcined at  $800^\circ\text{C}$  in the presence of air. Thus  $\text{Y}_{0.85}\text{Gd}_{0.15}\text{CrO}_3$  nanoparticles are produced using sol-gel method. We have used the sample name as S1 for the  $\text{Y}_{0.85}\text{Gd}_{0.15}\text{CrO}_3$  sample.

## 3. Results and discussions

### 3.1 XRD and TEM study

X ray diffraction pattern for  $\text{Y}_{0.85}\text{Gd}_{0.15}\text{CrO}_3$  sample is displayed in figure1. Prominent peaks in this figure represent different ( $hkl$ ) planes of  $\text{YCrO}_3$  and it also follows with ICDD PDF Number 34-0365 and not as an independent document.

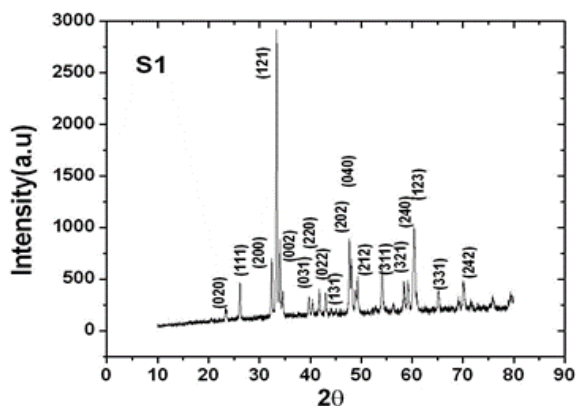
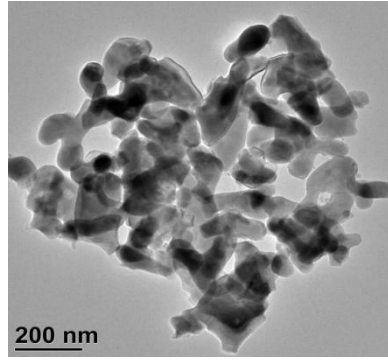


FIG.1 XRD pattern of S1 sample.

The typical TEM image of S1 sample has been displayed in figure 2. Average particle size has been calculated which results as 37 nm.



**FIG.2** TEM image of S1 sample

### 3.2 Dielectric Permittivity study

For the S1 sample the capacitance (C) and dissipation factor (D) are measured in the span of 20 Hz – 2 MHz. We have measured the real part and imaginary part of dielectric permittivity following the relations

$$\varepsilon' = \frac{Cd}{\varepsilon_0 A} \quad (1)$$

$$\varepsilon'' = \varepsilon' D \quad (2)$$

Where  $\varepsilon'$  and  $\varepsilon''$  represent the real part and imaginary part,  $\varepsilon_0$  represents the free space permittivity,  $A$  denotes electrode area and  $d$  is sample thickness. For the sample S1 the variation of  $\varepsilon'(f)$  and  $\varepsilon''(f)$  with respect to frequency at various temperatures are depicted in figure 3(a) and figure 3(b).

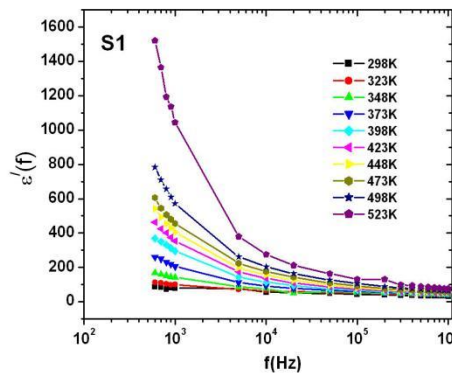


**FIG.3 (a)** The variation of the real part of permittivity with frequency for S1 sample.

It is clear from Fig.3(a) and 3(b) that both the real and imaginary part are strongly temperature dependent at higher temperature and lower frequency. At lower frequency a larger variation of dielectric permittivity versus temperature has been noticed with respect to the higher-frequency part. When the frequency is lower, the electronic, ionic, orientational and interfacial polarization [15-17] all give their contribution to the dielectric constant. At larger frequency the electric dipoles rotate slowly so the dipole oscillation delays

behind the applied field. As a result the orientational polarization diminishes as the dipoles are unable to follow the applied field. So due to the interfacial and space charge polarization dielectric permittivity decreases at high-frequency region [18-19].

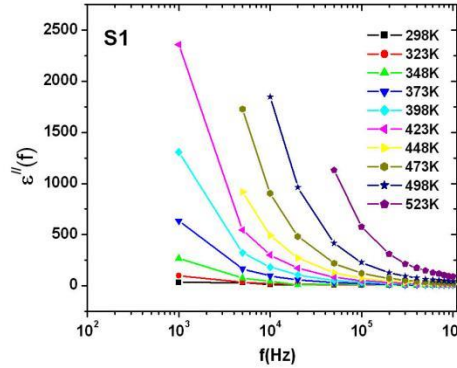


**FIG.3(b)** The frequency dependence of the imaginary part of permittivity for individual temperatures for S1 sample.

### 3.2 Electric Modulus study

For a disordered material hopping of charge carriers is successful when it is pursued by the polarization cloud surrounding the charge carriers [20]. Electric relaxation time  $\tau$  is required for the motion of the charge and the concomitant polarization cloud. Following this the dielectric characteristics of our sample may be analysed using complex electric modulus formalism [21]. Electric modulus ( $M^*$ ) is written below

$$M^* = \frac{1}{\varepsilon^*} = M' + iM'' \quad (3)$$

Where  $M'$  represents the real part and  $M''$  represents the imaginary part of dielectric modulus.

$M'$  and  $M''$  can be written as

$$M' = \frac{\varepsilon'}{\varepsilon'^2 + \varepsilon''^2} \quad (4)$$

$$M'' = \frac{\varepsilon''}{\varepsilon'^2 + \varepsilon''^2} \quad (5)$$

The relaxation time for the inclination of dipoles can be estimated from  $M''$ . The frequency variation of the real part of electric modulus has been shown in figure 4(a) for various temperatures and there does not exist any characteristic peak. In Fig.4(b) the frequency variation of  $M''$  is depicted for individual temperatures for S1 sample.

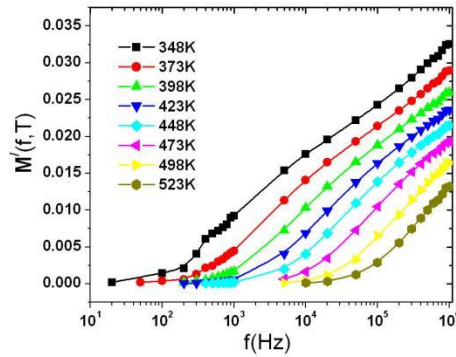


**FIG.4(a)** The frequency dependence of  $M''$  for different temperatures for S1 sample.

A loss peak is seen for individual temperatures. This happens for the interfacial polarization for a certain frequency range. As the temperature is increased the relaxation peaks shifts their position to the larger frequency side. For a certain temperature influenced by the applied field, the intrinsic immobilized charges (free) transfer easily as no obstacle is there. The dielectric disagreement between the surface shell and the core material produces interfacial polarization. This occurs as the free charges cannot move at the nanocrystals surface. With the increasing temperature, the motion of the charge carrier is increased due to accumulation of charge (free) at the interface. With the increasing mobility of charge carries, relaxation time is decreased. The loss peak shifts to the direction of the higher frequency part as the temperature increases.

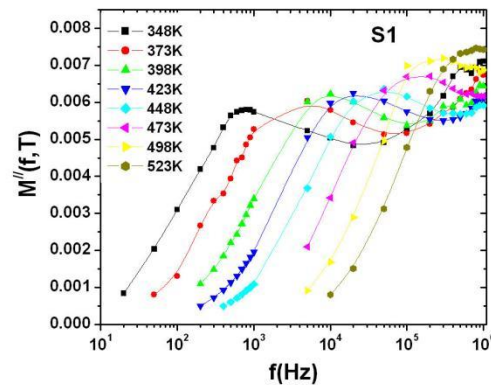


**FIG.4(b)** The frequency variation of  $M''$  for various temperatures for S1 sample.

The normalized plotting of  $M'' / M''_{\max}$  verses  $\ln \left[ \frac{f}{f_{\max}} \right]$  is depicted in figure 5 for S1 sample for different temperatures. It has been noticed that the spectra of  $M'' / M''_{\max}$  for individual temperatures combine into a whole on a single master curve. It concludes that all the dynamic procedure executing at various temperatures shows likely same activation energy.

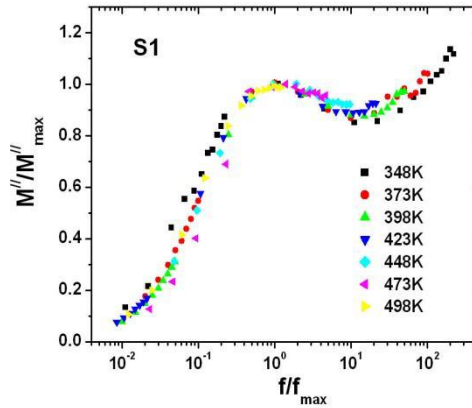


**FIG.5** The normalized plotting of  $\left( M'' / M''_{\max} \right)$  versus  $\left( \frac{f}{f_{\max}} \right)$  of S1 sample at different temperatures.

The average activation energy ( $E_{ar}$ ) which contributes to the relaxation nature may be estimated by analysing the temperature dependence of the relaxation time obeying the Arrhenius law written as

$$\tau = \tau_0 \exp\left(\frac{E_{ar}}{k_B T}\right) \tag{6}$$

Where  $\tau_0$  and  $E_{ar}$  represent pre exponential factor and activation energy. The value of activation energy is 0.33 eV which has been calculated from figure 6 for this sample.

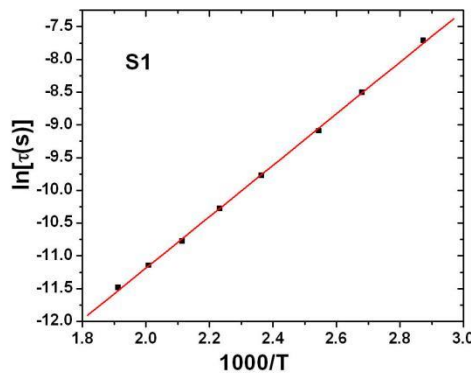


**FIG.6** The plotting of  $\ln(\tau)$  with  $1000/T$

The temperature dependence of relaxation time is given in Table 1. It has been noticed that the relaxation time is decreased with the increasing temperature.

**Table 1.** Temperature variation of Relaxation Time

Temperature(K)	Relaxation Time(s)
348	$1.4 \times 10^{-3}$
373	$4.07 \times 10^{-4}$
393	$1.12 \times 10^{-4}$
423	$5.11 \times 10^{-5}$
448	$2.20 \times 10^{-5}$
473	$9.07 \times 10^{-6}$
498	$5.73 \times 10^{-6}$
523	$2.28 \times 10^{-6}$

#### 4. Conclusion

Gd doped yttrium chromate nanoparticles have been prepared using sol-gel method. Characterization is done by XRD and TEM confirming the formation of nanoparticles. The frequency dependence of dielectric permittivity is measured for various temperatures. The electric modulus formalism is studied in detail and activation energy is estimated.

#### 5. Acknowledgements

The contribution and cooperation of Asansol Engineering College is gratefully acknowledged.

#### REFERENCES

- [1] A. J. Freeman, H. Schmid, Proceedings of the MEIPIC-1, Magnetoelectric Interaction Phenomena in Crystals (1975).
- [2] H. Schmid, A. Janner, H. Grimmer, J. P. Rivera and Z. G. Ye, Proceedings of the MEIPIC-2, Ferroelectrics (1994).
- [3] M. Bichurin, Proceedings of the MEIPIC-3, Ferroelectric(1997).
- [4] P. Curie, J. Physique 3 393(1894).
- [5] G. Lawes, J. Nanophotonics 2 (2008) 020306.
- [6] I. V. Oryshich, N. E. Poryadchenko, N. D. Bega, A. N. Rakitakii, Poroshk. Metall. 3–4 36(1996).
- [7] T. R. Armstrong, J. L. Bates, G. W. Coffey, L. R. Pederson, P. J. Raney, J. W. Stevenson, W. J. Weber, F. Zheng, Proc. 10th Annu. Conf. Fossil Energy Materials, p- 301(1996).
- [8] E. M. Levin, C. R. Robbins, H. F. McMurdie, Phase Diagrams for Ceramists, Vol. 3, American Ceramic Society, Columbus, p-143(1975).
- [9] T. Tachiwaki, Y. Kunifusa, M. Yoshinaka, K. Hirota, O. Yamaguchi, Int. J. Inorg. Mater. 3 107(2001).
- [10] J. H. Kim, H. S. Shin, S. H. Kim, J. H. Moon, B. T. Lee, Jpn. J. Appl. Phys. 42 575(2003).
- [11] A. N. Kamlo, J. Bernard, C. Lelievre, D. Houivet, J. Eur. Ceram. Soc. 31 1457(2011).
- [12] M. Kagawa, Y. Kato, Y. Syono, J. Aerosol Sci. 28 475(1997).

- 
- [13] K. J. Yoon, J. W. Stevenson, O. A. Marina, J. Power Sources 196, 8531(2011).  
[14] S. Wang, B. Lin, Y. Dong, D. Fang, H. Ding, X. Liu, G. Meng, J. Power Sources 188(2009)  
[15] K. K. Srivastava, A. Kuma, O. S. Panwar, L. N. Lakshminarayan, J. Non-Cryst. Solids 33, 205(1979).  
[16] B. Tareev, Physics of Dielectric Materials, Mir Publishers, Moscow (1975).  
[17] R. Ertugrul, A. Tataroghi, Chin. Phys. Lett. 29, 077304 (2012).  
[18] P. H. Bell, W. P. Davey, J. Chem. Phys. 9, 441(1941).  
[19] H. Frohlich, Theory of Dielectrics, Oxford University Press, London (1958).  
[20] J. B. M. Krishna, A. Saha, G. S. Okram, A. Soni, S. Purakayastha, and B. Ghosh, J. Phys. D: Appl. Phys. 42, 095404 (2009).  
[21] N. G. McCrum, B. E. Read, and G. Williams, An Elastic and Dielectric Effects in Polymeric solids, John Wiley and Sons, New York (1967).